DESIGN CONSIDERATIONS FOR A DUAL-FREQUENCY RADAR FOR SEA SPRAY MEASUREMENT IN HURRICANES

Daniel Esteban-Fernandez, Stephen L. Durden, Julian Chaubell, and Kenneth B. Cooper

Jet Propulsion Laboratory, California Institute of Technology

ABSTRACT

Over the last few years, researchers have determined that sea spray from breaking waves can have a large effect on the magnitude and distribution of the air-sea energy flux at hurricane-force wind speeds. Characterizing the fluxes requires estimates of the height-dependent droplet size distribution (DSD). Currently, the few available measurements have been acquired with spectrometer probes, which can provide only flight-level measurements. As such, in-situ measurement of near-surface droplet fluxes in hurricanes with these instruments is, at best, extremely challenging, if at all possible. This paper describes an airborne dual-wavelength radar profiler concept to retrieve the DSD of sea spray.

Index Terms— Sea spray, atmospheric radar, hurricane

1. INTRODUCTION

Of several factors contributing to hurricane intensity, air-sea interaction and specifically the effect of sea spray, are poorly understood [1]. The fundamental parameter required for characterizing the impact of sea spray on air-sea exchange processes is the size dependent *source function* for droplets, or the number of droplets of a given size produced at the sea surface per unit surface area per unit time as a function of wind speed. However, the extreme environment makes measurement of either the source function or the droplet size distribution (DSD) as a function of height, $n(r, z)$, extremely challenging. Instead, remote-sensing radar techniques are uniquely suited to tackle this problem. Specifically, multiple millimeter-wave frequencies are sensitive to small particles and can provide particle size information. The objective of this paper is to present the results of a feasibility study for a dual-wavelength Air-sea Spray Profiler (termed ASAP) that could be deployed both in manned aircrafts (such as C-130, WP-3 or similar) and in unmanned aerial vehicles (UAVs).

2. RADAR MEASUREMENT CONCEPT

2.1. Dual-frequency radar measurements

We would like to use radar to measure droplet size distribution parameters that can, in turn, be used to estimate heat and moisture flux for hurricane research. To get information about the DSD, we need at least two parameters of the DSD and, therefore, at least two radar measurements [2], [3]. To understand what a dual-frequency spray radar may measure, we couple backscattering calculations with the source function and DSD profile model of Fairall et al. [4]. Only droplets produced by spume are considered here. These droplets range from a few μm to nearly 1 mm. Smaller droplets produced by other mechanisms have an extremely small radar cross section. The sea spray droplets are assumed to be salt water; the dielectric function of Meissner and Wentz [5] is used. Since sea spray particle diameters are typically well below 1 mm, 94 GHz backscatter would be strongly dominated by Rayleigh scattering. Radar technology is also well-developed, making it a good choice for the lower frequency. The second, higher frequency is chosen to provide a non-Rayleigh frequency, as needed for dual-frequency measurements [3].

Figure 1 presents calculations for 35 m/s winds (a Category 1 Hurricane). Near the surface, the backscatter and differential reflectivity are high, and achieving a good SNR should not be too difficult. However, both signals decrease as altitude increases, due to the reduction in large particles. A threshold of 1 dB at roughly 100 m above the ocean surface is taken as a reasonable minimum differential reflectivity that should be successfully resolved by a dual-frequency radar system (when accounting for all sources of errors). Figure 1 differential reflectivity indicates that a 94/140 GHz system would be useful only for wind speeds roughly above 50 m/s, and would see only the lowest 250 m even at wind speeds as high as 60 m/s. On the other hand, a 94/220 GHz radar system would enable retrievals roughly starting at 35 m/s, and would be able to profile up to 1 km above the ocean surface at 60 m/s wind speed. These results suggest that the radar should therefore operate at 94 GHz and at least 220 GHz. Calculations with 94 and 300 GHz show an even larger differential reflectivity; however, atmospheric attenuation at 300 GHz is also much larger than at 220 GHz, as discussed next.

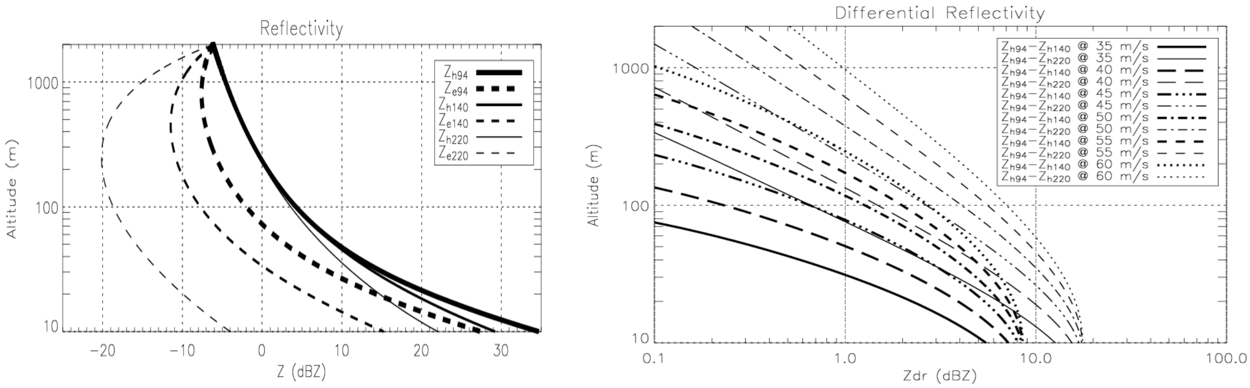

Figure 1. Lower left and right, radar reflectivity and differential reflectivity for 94, 140, and 220 GHz. The Z_e includes attenuation due to sea spray. These were derived for a wind speed of 35 m/s.

2.2. Effects of Attenuation

At high microwave frequencies, attenuation (mostly due to water vapor absorption) within the rain-free regions of hurricanes can limit sensitivity and increase the apparent differential reflectivity. In order to characterize the expected attenuation in a hurricane environment, we have used observations from GPS dropsondes that have been launched during hurricane reconnaissance flights, over different regions and several hurricane intensities. A dropsonde incorporates pressure, temperature, humidity sensor modules, as well as a GPS receiver module, and is therefore able to provide measurements of these quantities, including wind speed and direction, at an approximate rate of 2 Hz during the entire fall of the dropsonde. Liebe's model [6] has been used to derive an expected attenuation profile for each dropsonde profile. In order to quantify the mean attenuation that can be expected, all the retrieved attenuation profiles for a given hurricane flight in non-precipitating conditions (i.e., outside rain bands) have been averaged; its variability can then be estimated from the 68% confidence interval (1-sigma) of the attenuation profiles. The two-way path mean attenuation and 1-sigma variability for 94, 140, 220, and 300 GHz, assuming a flying altitude of 2 km, is 3.5 ± 1 dB, 8 ± 2.5 dB, 22 ± 4 dB, and 36 ± 7 dB, respectively. We choose 220 GHz for the second radar frequency, as a compromise between improving differential reflectivity and increasing attenuation. Transmit power using current technology is also higher at 220 GHz than at 300 GHz.

3. DSD, HEAT FLUX, AND ATTENUATION

3.1. Droplet-size distribution and heat flux retrieval

The retrieval algorithm, as previously mentioned, uses independent reflectivity measurements at two separate frequencies operating in different scattering regimes to derive the DSD of sea spray at several discrete altitudes above the ocean surface for the wind conditions observed. Here, as is commonly done in raindrop size distribution estimation, we assume that the DSD can be approximated by a gamma distribution. We developed an efficient procedure to fit the reflectivities predicted by the DSD to dual-frequency data. The retrievals were performed over a reflectivity profile, ranging from 30 m to 300 m, adding to the profiles four different levels of noise and performing the retrievals over 1000 noise realizations. From the retrieved spray DSD parameters, we used the method in [7] to derive sensible and latent heat flux.

3.2. Attenuation retrieval

The retrieval technique presented here has assumed that the unattenuated reflectivities are available at both frequencies. As shown in Section II-B, the attenuation due to water vapor can be quite large, potentially swamping the dual-frequency signal due to the particle size. Hence, accurate correction of attenuation must be accomplished prior to DSD retrieval. Our approach is to use a 37 GHz radiometer to estimate the water vapor attenuations at 94 and 220 GHz. To determine the feasibility of this approach we have developed a simple model for the brightness temperature of the ocean surface. The model also calculates the clear air attenuation at both 94 and 220 GHz. The slope of the 220 GHz attenuation versus the 37 GHz brightness temperature is roughly 0.5 dB per K for one-way attenuation. Since the radar reflectivity is affected by the two-way attenuation, this would be roughly 1 dB of differential reflectivity error for each K error in the radiometer measurement. Hence, sub-dB errors would require sub-K radiometer accuracy, along with accurate surface wind estimates. This is challenging, although feasible with current technology [8], [9].

4. RADAR SYSTEM DESIGN

The calculations in the previous section indicate that an airborne 94/220 GHz ASAP radar with a 37 GHz radiometer for attenuation correction can be used to measure sea spray water content, as well as sensible and latent heating. The requirements for ASAP are shown in Table 1. Two options for systems that meet these requirements have been investigated. The first is a traditional short pulse system. The pulse length is 60 ns, for a resolution of 9 m. The receiver noise figures are assumed to be 5 dB at 94 GHz and 8 dB at 220 GHz. The transmitters are assumed to be extended interaction klystrons, with peak power 1.5 kW at 94 GHz and 100 W at 220 GHz, based on currently available technology. Using the radar equation with a 0.5 second incoherent integration time and 40 cm diameter antenna, we find a minimum detectable reflectivity of -25 dBZ at 94 GHz and -37 dBZ at 220 GHz.

The pulse repetition frequency (PRF) for this option is 10000 Hz, allowing incoherent averaging of 5000 pulses during the integration time. Although the radar echoes themselves are not independent at this high PRF, the thermal noise added to these pulses is independent from pulse to pulse. Incoherent integration of many pulses allows an estimate of noise to be subtracted from the received signal plus noise, as done with CloudSat radar processing, for example [10]. At very low SNR the effective signal to noise improves as $\sqrt{N}$, where N is the number of pulses averaged. With these parameters, this radar design can meet requirements. Its implementation is straightforward at 94 GHz but challenging at 220 GHz due to the high power levels and required receiver isolation. Preventing receiver saturation or damage during each transmit event would require more than 50 dB isolation. This isolation can likely be achieved with a quasi-optical design [11] or with separate transmit and receive antennas. The quasi-optical design is preferable, since alignment of 40 cm antennas at 220 GHz is extremely difficult.

An option that eliminates the high power levels is a pulse compression radar system, using a linear, frequency modulated (FM) chirp [12]. The chirp bandwidth is 18 MHz, giving a range resolution of 8.4 m. We assume a solid-state transmitter with 100 mW peak power at 220 GHz; this lower power level can be handled by current switch technology. At W-band a 1 W solid state transmitter is used. These power levels are 30-35 dB below the powers assumed for the short pulse option. To make up for this loss, we keep a similar bandwidth but lengthen the pulse from 60 ns to 60 μs. This pulse length corresponds to a 9 km radar range. In conventional radar operation alternating between transmit and receive, a 9-km blind zone would occur during the transmit event. Since our nominal altitude is 2 km, the radar must receive while transmitting. This can be accomplished by separating transmit and receive antennas (undesirable, as explained above) or by using a quasi-optical circulator. At the expense of some power, a beam splitter can also be used to route half the transmit power to the receiver and half the receive power to the receiver. This results in a 6 dB loss but can be compensated by using an even longer pulse.

For pulse compression radars, range sidelobes from the ocean surface return can potentially obscure the reflectivity measurements at the lowest altitudes, thereby limiting the system's ability to retrieve the spray DSD down to the ocean surface. In FMCW radars (pulse compression with 100% duty cycle) this is the equivalent of phase noise due to a bright clutter target interfering with the desired target [13]. Currently, no measurements of ocean backscatter have been found reported in the literature for frequencies above W-band (94 GHz). Typically, ocean backscatter decreases weakly with increasing frequency. To be conservative, we take the 220 GHz backscatter to be the same as that at 94 GHz and use σ^0 as 10 dB. The surface return then exceeds the minimum detectable spray return by about 60 dB at 94 GHz and 50 dB at 220 GHz. Hence, system errors must be controlled to suppress the clutter (range sidelobes) from the surface to these levels [12].

5. LABORATORY DEMONSTRATION

A laboratory demonstration of a 220 GHz FMCW radar has been accomplished. It is based on an improved version of the terahertz radar described in [14]; the final frequency tripler has been removed to result in an output frequency near 220 GHz and the receiver mixer has been replaced with a sub-harmonic mixer that mixes the received signal down to a 3.6 GHz intermediate frequency (IF). This signal is IQ-detected by mixing with the transmitted chirp and Fourier transformed to change range to frequency.

The left panel in Figure 2 shows data for a 3 mm gold bead at 4.3 m range, while the center panel is the measurement of water spray from a spray dispenser at 4.3 m range. The nearly constant signal at 1-2 m range is transmit/receive leakage. The radar bandwidth is 5.3 GHz, corresponding to a 3 cm range resolution, while the beam is approximately 1 cm wide at the target. The geometrical optics cross section of the gold sphere can be used to infer that the spray equivalent radar reflectivity is 10-20 dBZ, well above the worst case spray reflectivity assumed in the previous section. A nearly 60 dB difference between the peak return for the sphere and noise a few meters away is seen (right panel, 8 m range). A target at a range of 2 km would tend to create larger clutter due to phase noise than our point target at 4.3 m, due to the cancellation of phase errors when mixing the transmit and receive signals for short-range targets [13].

6. ACKNOWLEDGMENTS

The research presented in the paper was carried out at the Jet Propulsion Laboratory, California Institute of

Technology, under contract with the National Aeronautic and Space Administration. Support from the JPL Research and Technology Development (R&TD) program and from NASA Earth Science Technology Office (ESTO) is gratefully acknowledged.

7. REFERENCES

[1] E. L. Andreas, "Spray stress revisited," *J. Phys. Oceanogr*., vol. 34, no. 6 pp. 1429-1440, 2004.

[2] Z. S. Haddad, E. Im, and S. L. Durden, "Intrinsic ambiguities in the retrieval of rain rates from radar returns at attenuating wavelengths," *J. Appl. Meteor*., vol. 34, no. 12, pp. 2667-2679, 1995.

[3] R. J. Hogan and A. J. Illingworth, "The potential of spaceborne dual-wavelength radar to make global measurements of cirrus clouds," *J. Atmos. Oceanic Technol.*, vol. 16, pp. 518-531, 1999.

[4] C. W. Fairall, M. L. Banner, W. L. Peirson, W. Asher, and R. P. Morison "Investigation of the physical scaling of sea spray spume droplet production," *J. Geophys. Res.*, vol. 114, doi:10.1029/2008JC004918, 2009.

[5] T. Meissner and F. J. Wentz, "The complex dielectric constant of pure and sea water from microwave satellite observations," *IEEE Trans. Geosci. Remote Sensing*, vol. 42, pp. 1836-1849, 2004.

[6] H. B. Liebe, "MPM93 – Propagation model of moist air at frequencies below 1000 GHz," AGARD Conf. Proceedings No. 495, 1993.

[7] E. L. Andreas and J. DeCosmo, "Sea spray production and influence on air–sea heat and moisture fluxes over the open ocean," in Geernaert, G. L., editor, *Air–seaexchange: physics, chemistry and dynamics*, pp. 327–362. Kluwer Academic Publishers, Dordrecht, 1999.

[8] J.P. Bobak, B.C. Hicks, L.A. Rose et al., "APMIR: an airborne polarimeter designed for high accuracy," *IEEE Proc. Oceans*, vol. 1, pp. 211-216, 2003.

[9] E. W. Uhlhorn, P. G. Black, J. L. Franklin, M. Goodberlet, J. Carswell, and A. S. Goldstein, "Hurricane surface wind measurements from an operational stepped frequency microwave radiometer," *Mon. Wea. Rev.,* vol. 135, no. 9, pp. 3070-3085, 2007.

[10] S. Tanelli, S. L. Durden, E. Im, K. Pak, D. Reinke, P. Partain, J. Haynes, R. Marchand, "CloudSat's Cloud Profiling Radar after two years in orbit: performance, calibration, and processing," *IEEE Trans. Geosci. Remote Sensing*, vol. 46, no. 11, pp. 3560-3573, Nov. 2008.

[11] Derek H. Martin and Richard J. Wylde, "Wideband Circulators for Use at Frequencies Above 100 GHz to Beyond 350 GHz," *IEEE Trans. Microw. Theory Tech*., vol. 57, no. 1, Jan 2009.

[12] A. Tanner, S. L. Durden, R. Denning, E. Im, F. K. Li, W. Ricketts, W. Wilson, "Pulse compression with very low sidelobes in an airborne rain mapping radar," *IEEE Trans. Geosci. Remote Sensing*, vol. 32, no. 1, pp. 211-213, 1994.

[13] P. D. L. Beasley, "The influence of transmitter phase noise on FMCW radar performance," *Proc. 3rd European Radar Conf.*, 2006.

[14] K. B. Cooper et al., "A High-Resolution Imaging Radar at 580 GHz," *IEEE Trans. Micro. Wireless Comp. Lett*., vol. 18, pp. 64-66, 2008.

Table 1. Requirements for Air Sea Spray Profiler (ASAP)

Radar Parameter	Requirement	Rationale
Frequency 1	94 GHz	High enough to get good sensitivity with small particles; low enough to be primarily in Rayleigh regime; proven technology
Frequency 2	220 GHz	High enough to give observable differential reflectivity (non-Rayleigh) but low enough to have acceptable attenuation
Radiometer frequency	37 GHz	Allow compact implementation with high accuracy and stability
Platform altitude	2000 m	Minimize range to spray but maintain safe altitude
Minimum detectable reflectivity	-25 dBZ @ 94 GHz -35 dBZ @ 220 GHz	Detection of sea spray over range of winds with attenuation, based on calculated reflectivities
Max horizontal resolution	50 m (instantaneous)	Resolve likely inhomogeneity of spray
Max vertical resolution	10 m	Most spray in lowest 100 m
Absolute accuracy	1 dB	Accuracy in retrieved water content
Relative accuracy	0.4 dB	Accuracy in retrieved water content
Attenuation correction accuracy	0.1 dB (0.1 K brightness temperature measurement)	Differential attenuation must be corrected for accurate dual-frequency retrievals
Dynamic range	90 dB	Accommodate return from spray and from ocean surface

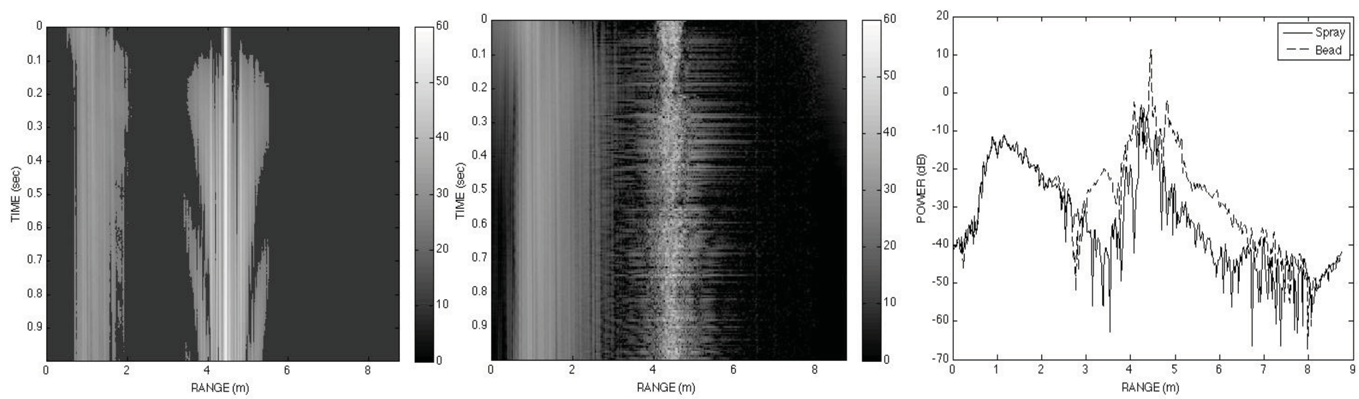

Figure 2. FMCW time–range images of a 3 mm gold bead (left) and water spray (center), in relative (uncalibrated) power in dB scale. At right is a horizontal cut through both left and center data, showing received power versus range.